

ZD1839 induces p15^{INK4b} and causes G₁ arrest by inhibiting the mitogen-activated protein kinase/extracellular signal-regulated kinase pathway

Makoto Koyama, Youichirou Matsuzaki, Shingo Yogosawa, Toshiaki Hitomi, Mayumi Kawanaka, and Toshiyuki Sakai

Department of Molecular-Targeting Cancer Prevention, Graduate School of Medical Science, Kyoto Prefectural University of Medicine, Kawaramachi-Hirokoji, Kamigyo-ku, Kyoto, Japan

Abstract

Inactivation of the retinoblastoma protein pathway is the most common abnormality in malignant tumors. We therefore tried to detect agents that induce the cyclin-dependent kinase inhibitor p15^{INK4b} and found that ZD1839 (gefitinib, Iressa) could up-regulate p15^{INK4b} expression. ZD1839 has been shown to inhibit cell cycle progression through inhibition of signaling pathways such as phosphatidylinositol 3'-kinase-Akt and mitogen-activated protein kinase (MAPK)/extracellular signal-regulated kinase (ERK) cascades. However, the mechanism responsible for the differential sensitivity of the signaling pathways to ZD1839 remains unclear. We here showed that ZD1839 up-regulated p15^{INK4b}, resulting in retinoblastoma hypophosphorylation and G₁ arrest in human immortalized keratinocyte HaCaT cells. p15^{INK4b} induction was caused by MAPK/ERK kinase inhibitor (PD98059), but not by Akt inhibitor (SH-6, Akt-III). Moreover, mouse embryo fibroblasts lacking p15^{INK4b} were resistant to the growth inhibitory effects of ZD1839 compared with wild-type mouse embryo fibroblasts. Additionally, the status of ERK phosphorylation was related to the antiproliferative activity of ZD1839 in human colon cancer HT-29 and Colo320DM cell lines. Our results suggest that induction of p15^{INK4b} by inhibition of the MAPK/ERK pathway is associated with the antiproliferative effects of ZD1839. [Mol Cancer Ther 2007;6(5):1579–87]

Received 12/31/06; accepted 3/15/07.

Grant support: Grant-in-Aid from the Japanese Ministry of Education, Culture, Sports, Science, and Technology, and a Grant-in Aid for the Encouragement of Young Scientists from the Japan Society for the Promotion of Science.

The costs of publication of this article were defrayed in part by the payment of page charges. This article must therefore be hereby marked *advertisement* in accordance with 18 U.S.C. Section 1734 solely to indicate this fact.

Requests for reprints: Toshiyuki Sakai, Department of Molecular-Targeting Cancer Prevention, Graduate School of Medical Science, Kyoto Prefectural University of Medicine, Kawaramachi-Hirokoji, Kamigyo-ku, Kyoto 602-8566, Japan. Phone: 81-75-251-5339; Fax: 81-75-241-0792. E-mail: tsakai@koto.kpu-m.ac.jp

Copyright © 2007 American Association for Cancer Research.

doi:10.1158/1535-7163.MCT-06-0814

Introduction

Cell cycle regulation is important in growth control, and therefore the deregulation of cell cycle machinery has been implicated in carcinogenesis (1). Cyclins and cyclin-dependent kinases (CDK), in association with each other, play key roles in promoting the G₁-to-S phase transition of the cell cycle by phosphorylating the retinoblastoma (RB) protein (2, 3). Activation of cyclin-CDK complexes is counterbalanced by CDK inhibitors including the INK4 family. The INK4 family consists of p15^{INK4b}, p16^{INK4a}, p18^{INK4c}, and p19^{INK4d}, and their members, with similar affinity, are specific inhibitors of cyclin D-CDK4/6 complexes (4, 5).

A great number of cancer studies have shown that most of the abnormalities leading to malignancies involve inactivation of tumor suppressor molecules, such as the INK4 family, associated with the RB pathway (6, 7). Consistently, for example, mice deficient in p16^{INK4a} or p18^{INK4c} are highly susceptible to various types of malignant tumors (8–10). In many malignant tumors, p16^{INK4a} is inactivated by homozygous deletions, gene methylation, or mutations (11, 12). In contrast to p16^{INK4a}, alterations of p15^{INK4b}, p18^{INK4c}, and p19^{INK4d} genes are rare events in malignant tumors, although these genes have functions similar to that of p16^{INK4a} (6). Regarding the association between p15^{INK4b} and carcinogenesis, p15^{INK4b} is an essential mediator in cell cycle arrest in response to cytostatic signals (13). The p15^{INK4b} gene is one of the major target genes in an oxidative stress-induced rat renal carcinogenesis model (14). There is also a significant relationship between p15^{INK4b} methylation and overall survival of patients with non-small-cell lung cancer (15). We therefore have focused on p15^{INK4b} as a member of the INK4 family and have found that the histone deacetylase inhibitor trichostatin A causes G₁ arrest by inducing p19^{INK4d} (16) and p18^{INK4c} (17), and that trichostatin A (18) and a naturally occurring compound, indole-3-carbinol (19), up-regulate p15^{INK4b}, resulting in hypophosphorylation of the RB protein. Moreover, we previously established the screening system to detect p15^{INK4b}-inducing agents using a branched-DNA assay. As a result, we found several p15^{INK4b} inducers, including an agent whose structural formula is similar to that of ZD1839, and a pyridopyrimidine derivative as a novel mitogen-activated protein kinase (MAPK)/extracellular signal-regulated kinase (ERK) kinase (MEK)-1/2 inhibitor.¹ We subsequently confirmed that ZD1839 also induces p15^{INK4b} expression. ZD1839 has been shown to block epidermal growth factor receptor

¹ Yamaguchi et al., submitted for publication.

(EGFR) phosphorylation and its downstream pathways such as phosphatidylinositol 3'-kinase (PI3K)-Akt and MAPK/ERK cascades, resulting in inhibition of proliferation in tumor cell lines (20–22). EGFR is expressed in most human tissues and is often highly expressed in human solid tumors (23, 24). However, the level of EGFR expression alone is not sufficient to predict the response of tumor cells to ZD1839 (25, 26). Several groups have shown that ZD1839 effectively induces a marked response in patients with non-small-cell lung cancer who have somatic mutations in exons 18 to 21 in the ATP-binding region of the EGFR kinase domain (27–29). These findings indicate that EGFR mutations might be a determinant of ZD1839 sensitivity in non-small-cell lung cancer. On the other hand, activating EGFR mutations are rare in colorectal cancer, and patients whose colorectal cancer possessed no EGFR mutations experienced disease regression following treatment with ZD1839 and chemotherapy (30). Therefore, other downstream events may influence responsiveness to EGFR inhibition.

We here show that ZD1839 induces p15^{INK4b} by inhibiting ERK phosphorylation, and that p15^{INK4b} status is at least partially associated with ZD1839 sensitivity. We suggest for the first time that the ability of ZD1839 to induce p15^{INK4b} by inhibiting signals through the MAPK/ERK pathway could be one of the mechanisms of the antiproliferative activity of this agent.

Materials and Methods

Cell Culture and Reagents

Human immortalized keratinocyte HaCaT cells (a kind gift from Dr. N.E. Fusenig, German Cancer Research Center, Heidelberg, Germany) and human colon cancer cell lines (HT-29 and Colo320DM) were maintained in DMEM containing 10% fetal bovine serum, 2 mmol/L glutamine, and antibiotics (penicillin/streptomycin), and were incubated at 37°C in a humidified atmosphere with 5% CO₂. Wild-type and p15^{INK4b}-deficient [p15(-/-)] mouse embryo fibroblasts (MEF; ref. 9; a kind gift from Dr. Paul Krimpenfort, Division of Molecular Genetics and Centre of Biomedical Genetics, Netherlands Cancer Institute, Amsterdam, the Netherlands) were maintained in DMEM supplemented with 10% fetal bovine serum, 2 mmol/L glutamine, 0.1 mmol/L MEM nonessential amino acids, 55 mmol/L 2-mercaptoethanol, and antibiotics (penicillin/streptomycin), and incubated at 37°C in a humidified atmosphere of 9% CO₂. ZD1839 (Gefitinib, Iressa) was supplied by AstraZeneca. PD98059 (MEK inhibitor) and Akt-III (SH-6; Akt inhibitor) were purchased from Calbiochem. They were dissolved in DMSO and diluted to the final concentration in each volume of culture medium used.

Growth Inhibition Assay and Cell Cycle Analysis

One day after inoculation of cells, various concentrations of ZD1839, PD98059, or Akt-III were added to the culture medium. The number of viable cells was counted 24 to 48 h after drug addition with the trypan blue dye exclusion

test. For flow cytometry analysis, unsynchronized HaCaT cells were exposed to the agents for the indicated times. The cells were then treated with Triton X-100 and RNase A, and their nuclei were stained with propidium iodide before DNA content was measured using a Becton Dickinson FACSCalibur. At least 10,000 cells were counted and the ModFit LD V2.0 software package (Becton Dickinson) was used to analyze the data.

RNA Isolation and Northern Blot Analysis

Total RNA was isolated using a Sepasol RNA isolation kit (Nacalai Tesque, Inc.) and poly(A)⁺ mRNA was separated from 200 µg of total RNA using an Oligotex-dT30 (Super) mRNA purification kit (Takara Bio, Inc.). Poly(A)⁺ mRNA was fractionated on 1% agarose gels, transferred to nylon filters, and probed according to standard procedures. Exon 1 of p15 cDNA was used as a probe. Northern blot analysis was done using standard methods (31). For mRNA half-life studies, 5 µg/mL actinomycin D (Sigma) was added directly to the medium. The relative band intensity was assessed by densitometric analysis of digitalized autographic images using Scion Image software (Scion Corp.).

Protein Isolation and Western Blot Analysis

Cells were lysed in lysis buffer [50 mmol/L Tris-HCl (pH 7.5), 1% SDS]. The protein extract was then boiled for 5 min and loaded onto a 12% (for p15^{INK4b}, p16^{INK4a}, p18^{INK4c}, p19^{INK4d}, p21^{WAF1}, p27^{KIP1}, c-myc, cyclin D1, CDK4/6, and α-tubulin detection) or a 10% [for phospho-Akt, Akt, phospho-p42/44 MAPK (p-ERK1/2), p42/44 MAPK (ERK1/2), and phospho-GSK3β detection] or a 7% (for RB detection) polyacrylamide gel, subjected to electrophoresis, and transferred to a nitrocellulose membrane. The following antibodies were used as the primary antibody: rabbit anti-human p15^{INK4b} polyclonal antibody (C-20, Santa Cruz Biotechnology, CA), mouse anti-human p16^{INK4a} monoclonal antibody (mAb; G175-1239, PharMingen), rabbit anti-human p18^{INK4c} polyclonal antibody (N-20, Santa Cruz Biotechnology), mouse anti-human p19^{INK4d} mAb (2D2G4, Zymed Laboratories), mouse anti-human p21^{WAF1} mAb (6B6, PharMingen), rabbit anti-human p27^{KIP1} polyclonal antibody (C-19, Santa Cruz Biotechnology), mouse c-myc mAb (9E10, Santa Cruz Biotechnology), CDK4 mAb (H-22, Santa Cruz Biotechnology), mouse anti-human CDK6 mAb (DCS-83, MBL), mouse anti-human pRB mAb (G3-245, PharMingen), rabbit anti-human Akt, phospho-Akt (Ser⁴⁷³), phospho-p42/44 MAPK, p42/44 MAPK, phospho-GSK3β (Ser⁹) antibody (phospho-Akt Pathway Sampler Kit, Cell Signaling Technology, Inc.), and α-tubulin antibody (Oncogene Research Products). The signal was then developed with an enhanced chemiluminescence system (Amersham Pharmacia Biotech, UK Ltd.).

Cell Viability Assay

Cells were seeded at 4,000 per well in 96-well plates. The number of viable cells was determined by Cell Counting Kit-8 assay according to the manufacturer's instructions (Dojindo, Kumamoto, Japan). After incubation with the indicated concentrations of ZD1839 or PD98059, kit reagent WST-8 was added to the medium and incubated for a further 1 h. The absorbance of samples (450 nm) was

determined using a scanning multiwell spectrophotometer that serves as an ELISA reader.

Statistical Analysis

Statistical evaluation of the data was done using the Student's *t* test for simple comparison between groups and treatments. $P < 0.05$ was considered statistically significant.

Results

Cell Growth Inhibition and G₁ Arrest by ZD1839 in HaCaT Cells

We first investigated the antiproliferative effects of ZD1839 in human immortalized keratinocyte HaCaT cells. We observed that ZD1839 inhibits the growth of HaCaT cells in a dose-dependent manner and 600 nmol/L ZD1839 had a cytostatic effect (Fig. 1A). To examine the effects of ZD1839 on cell cycle progression, the DNA content of the cell nuclei was measured by flow cytometry analysis. The treatment with 600 nmol/L ZD1839 increased the percentage at the G₁ phase and decreased that at the S phase in a time-dependent manner (Fig. 1B). These data show that ZD1839 arrests the cell cycle of HaCaT cells at the G₁ phase.

p15^{INK4b} Induction and RB Hypophosphorylation by ZD1839 in HaCaT Cells

We tried to elucidate whether the expression of p15^{INK4b} protein could be influenced by treatment with ZD1839 in HaCaT cells. The time course study showed that p15^{INK4b} was markedly increased at 24 h or more after treatment with ZD1839 in a time-dependent manner, compared with the treatment with solvent DMSO alone (Fig. 1C). These results suggest that p15^{INK4b} is an important molecular target of ZD1839 among the INK4 family, whose members are associated with G₁ cell cycle arrest. There were no obvious changes in the abundance of other INK4 family members such as p16^{INK4a}, p18^{INK4c}, and p19^{INK4d}; however, the expression of p21^{WAF1} and p27^{KIP1} was slightly up-regulated after treatment with ZD1839 as previously reported (32, 33). The protein p15^{INK4b} is a specific inhibitor of cyclin D-dependent kinases and the subsequent dephosphorylation of the RB protein causes G₁ cell cycle arrest. We therefore examined whether ZD1839 could alter the phosphorylation status of the RB protein in HaCaT cells. A hyperphosphorylated form of the RB protein (ppRB) was converted into a hypophosphorylated form (pRB) 24 to 48 h after the treatment (Fig. 1C). Taken together, these results indicate that ZD1839 up-regulates p15^{INK4b} protein levels and subsequently converts a hyperphosphorylated form of the RB protein into a hypophosphorylated form in HaCaT cells.

p15^{INK4b} mRNA Up-regulation by ZD1839 in HaCaT Cells

We next investigated in a time course study using Northern blot analysis whether ZD1839 could also affect p15^{INK4b} mRNA in HaCaT cells. The result indicated that p15^{INK4b} mRNA was up-regulated at 12 h or more after treatment with ZD1839 in a time-dependent manner (Fig. 2A). The longer transcript of p15^{INK4b} mRNA is ~3.2 kb and the shorter transcript is ~2.2 kb. These two transcripts were detected in a previous report (13). Because we found that p15^{INK4b} mRNA

is induced by ZD1839, we evaluated the effect of ZD1839 on the promoter activity in a p15^{INK4b} promoter-luciferase fusion plasmid by transient assay (18). However, we did not detect significant up-regulation of the p15^{INK4b} promoter by ZD1839

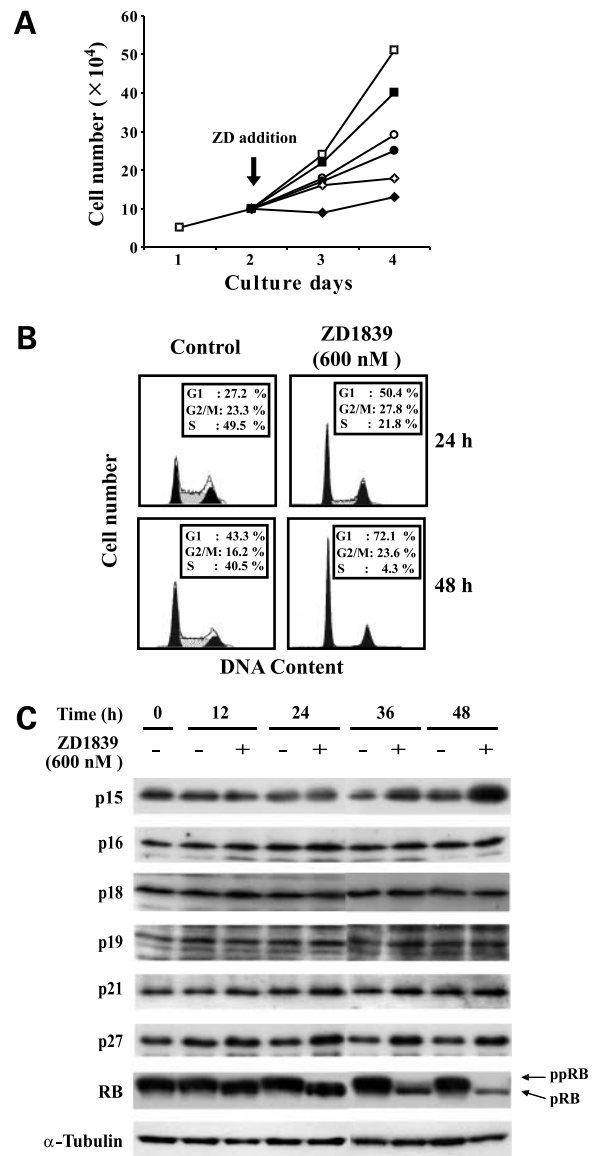


Figure 1. Effects of ZD1839 on cell growth and CDK inhibitors expression in HaCaT cells. **A**, one day after inoculation of HaCaT cells, ZD1839 at 50 (■), 100 (○), 200 (●), 400 (◇), or 600 (◆) nmol/L was added, and cell growth was compared with control treated with equivalent DMSO (□). The number of viable cells was counted by trypan blue dye exclusion test. Points, mean of duplicate experiments. **B**, unsynchronized HaCaT cells were incubated in the presence of either DMSO or 600 nmol/L ZD1839 for 24 h (top) and 48 h (bottom), and the DNA content of the cells was determined by flow cytometry. Data represent means of duplicate experiments. **C**, HaCaT cells were exposed either to DMSO alone (-) or to 600 nmol/L ZD1839 (+) for the indicated times. The expressions of INK4 family proteins (p15^{INK4b}, p16^{INK4a}, p18^{INK4c}, and p19^{INK4d}), CIP/KIP family proteins (p21^{WAF1} and p27^{KIP1}), and RB protein were analyzed by Western blotting. α-Tubulin was chosen as the loading control in all blots.

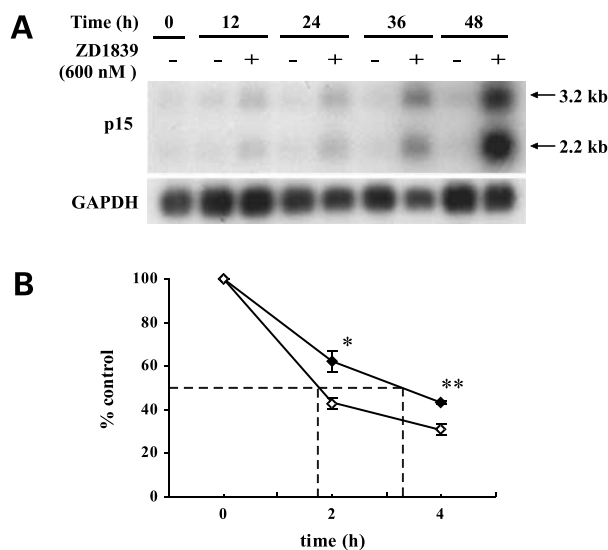


Figure 2. Effects of ZD1839 on p15^{INK4b} mRNA in HaCaT cells. **A**, HaCaT cells were exposed either to DMSO (–) or to 600 nmol/L ZD1839 (+). Total RNA was extracted at the indicated times, and the expression of p15^{INK4b} mRNA examined by Northern blot analysis. The same blot was hybridized with a glyceraldehyde-3-phosphate dehydrogenase (GAPDH) probe to normalize the amount of loaded mRNA. **B**, actinomycin D at 5 μg/mL was added to HaCaT cells followed by a 36-h incubation period in the presence or absence of 600 nmol/L ZD1839. At the indicated times after actinomycin D treatment, total RNA was isolated and p15^{INK4b} mRNA levels were examined by Northern blot analysis. The same blot was hybridized with a GAPDH probe to normalize the amount of loaded mRNA. The graph shows p15^{INK4b} mRNA levels in the presence (◆) or absence (◇) of 600 nmol/L ZD1839. The results were plotted as the ratio of the p15^{INK4b} mRNA level normalized to GAPDH mRNA levels present at time 0 of actinomycin D treatment. Points, mean of triplicate experiments; bars, SD. *, *P* < 0.05; **, *P* < 0.01, significantly different compared with DMSO-treated control.

(data not shown). To investigate whether a posttranscriptional regulation mechanism could be involved in p15^{INK4b} expression, we next did a series of mRNA half-life studies in HaCaT cells. Actinomycin D was added to HaCaT cells to prevent mRNA synthesis followed by a 36-h incubation period in the presence or absence of ZD1839. At the indicated times after actinomycin D treatment, p15^{INK4b} mRNA levels were examined by Northern blot analysis. The half-life of p15^{INK4b} mRNA was calculated to be 1.6 h in control cells. On the other hand, in cells treated with ZD1839, the half-life of p15^{INK4b} mRNA increased ~2-fold (3.2 h; Fig. 2B). These results suggest that an increase of p15^{INK4b} mRNA stability could at least partially contribute to the up-regulation of p15^{INK4b} by ZD1839.

Effects of ZD1839 on the Expression of Cell Cycle Regulatory Molecules in HaCaT Cells

We examined the effects of ZD1839 on the expression of cell cycle regulatory molecules in HaCaT cells. The time course study indicated that cyclin D1 and its transcription factor c-myc were down-regulated 12 h after treatment with ZD1839 (Fig. 3). Moreover, we investigated the effects of ZD1839 on the phosphorylation of EGFR downstream molecules, Akt and ERK, in HaCaT cells. The time course study indicated that ERK phosphoryla-

tion was down-regulated 12 h after treatment with ZD1839; however, no apparent change in phosphorylation of Akt and its downstream molecule GSK3β was observed (Fig. 3). These results suggest that the inhibition of ERK phosphorylation is involved in ZD1839-mediated cell cycle arrest of HaCaT cells.

Effects of Inhibiting Downstream Signals of EGFR

The MAPK/ERK and PI3K-Akt pathways are two main signaling pathways downstream of EGFR. We examined the effects of MEK inhibitor PD98059 and Akt inhibitor Akt-III on the cell cycle regulation and p15^{INK4b} induction in HaCaT cells. Both agents inhibited the cell growth in a dose-dependent manner (Fig. 4A) and increased the percentage at the G₁ phase and decreased that at the S phase, respectively (Fig. 4B). We then did Western blot analysis 48 h after treatment with 40 μmol/L PD98059 or 20 μmol/L Akt-III. PD98059 induced p15^{INK4b} and p27^{KIP1} and down-regulated c-myc. This pattern of the expression profile is similar to that observed with ZD1839 (Figs. 1C, 3, and 4C). Akt-III increased p21^{WAF1} and p27^{KIP1} and decreased cyclin D1 expression; however, unlike PD98059, Akt-III did not induce p15^{INK4b} (Fig. 4C). These results suggest that p15^{INK4b} induction is associated with the inhibition of the MAPK/ERK pathway in HaCaT cells.

Association between p15^{INK4b} or ERK Phosphorylation Status and the Antiproliferative Effects of ZD1839

To reveal whether p15^{INK4b} contributes to the antiproliferative activity of MEK inhibitor as a result of the

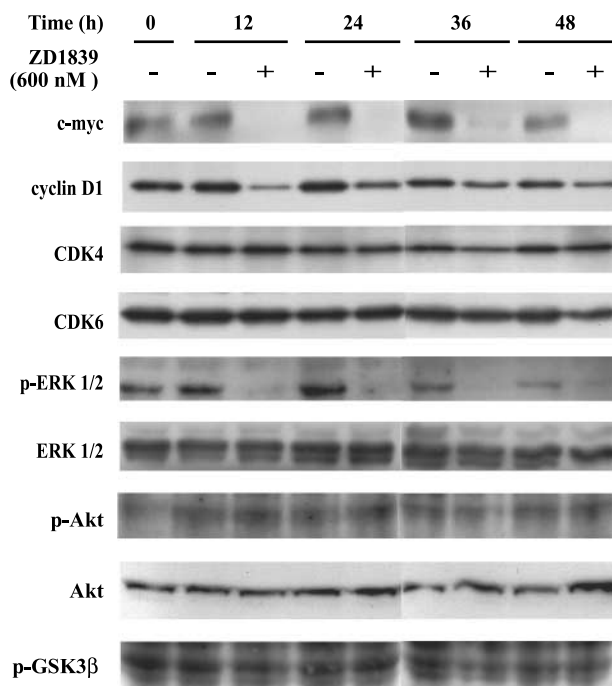
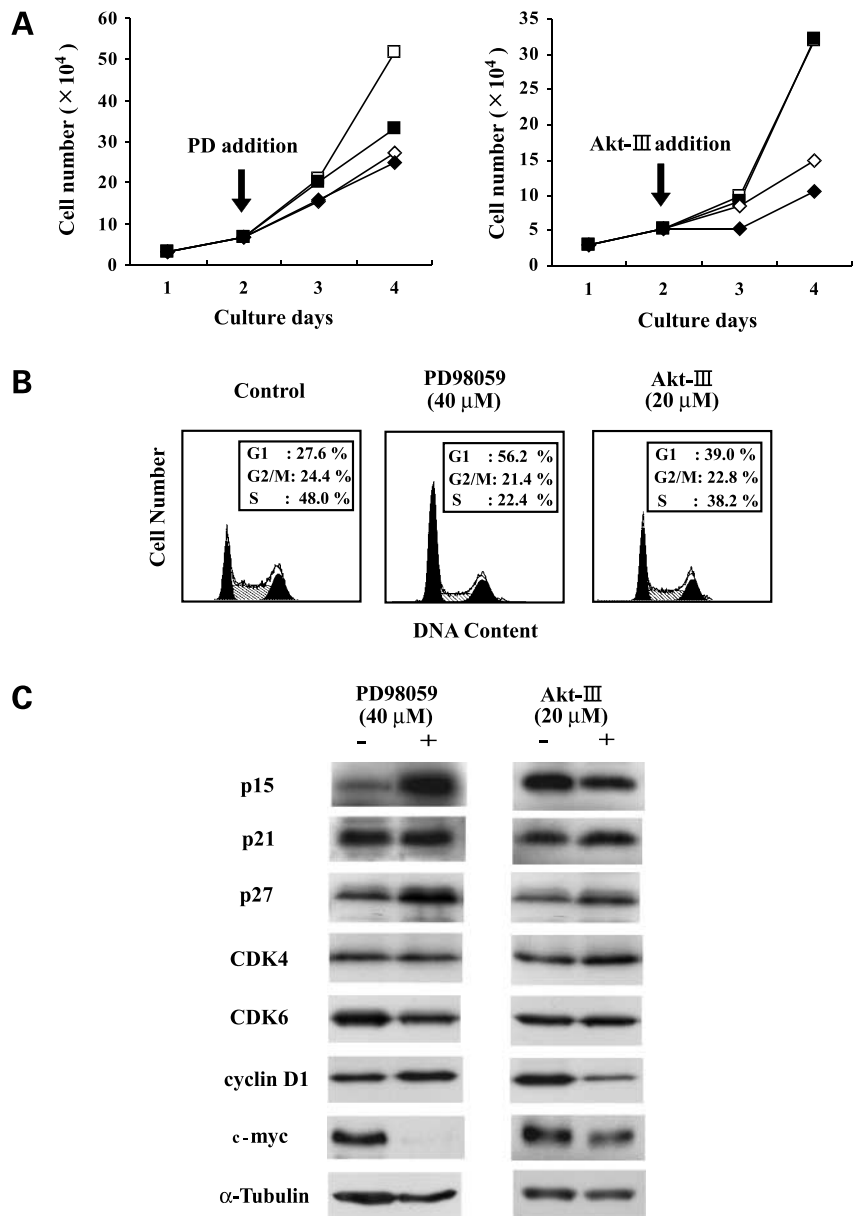


Figure 3. Effects of ZD1839 on the expression of cell cycle regulatory molecules in HaCaT cells. HaCaT cells were exposed to DMSO (–) or 600 nmol/L ZD1839 (+) for the indicated times. The expressions of c-myc, cyclin D1, CDK4/6, p-ERK1/2 (phospho-p42/44 MAPK), ERK1/2 (p42/44 MAPK), p-Akt (Ser⁴⁷³), Akt, and p-GSK3β (Ser⁹) proteins were examined by Western blotting.

Figure 4. Effects of the inhibition of the PI3K-Akt and MAPK/ERK pathways in HaCaT cells. **A**, one day after inoculation of HaCaT cells, PD98059 (*left*) at 10 (■), 20 (◇), or 40 (◆) $\mu\text{mol/L}$ or Akt-III (*right*) at 5 (■), 10 (◇), or 20 (◆) $\mu\text{mol/L}$ was added, and cell growth was compared with control treated with equivalent DMSO (□). The number of viable cells was counted by trypan blue dye exclusion test. *Points*, mean of duplicate experiments. **B**, unsynchronized HaCaT cells were incubated in the presence of DMSO (*left*), 40 $\mu\text{mol/L}$ PD98059 (*middle*), or 20 $\mu\text{mol/L}$ Akt-III (*right*) for 48 h, and the DNA content of the cells was determined by flow cytometry. Data represent means of duplicate experiments. **C**, HaCaT cells were exposed to DMSO alone (-) or to 40 $\mu\text{mol/L}$ PD98059 (+) or to 20 $\mu\text{mol/L}$ Akt-III (+) for 48 h. The expressions of p15^{INK4b}, p21^{WAF1}, p27^{KIP1}, CDK4/6, cyclin D1, and c-myc proteins were examined by Western blotting. α -Tubulin was chosen as the loading control in all blots.



inhibition of ERK phosphorylation, we did the Cell Counting Kit-8 assay to assess the viability of wild-type and p15^{INK4b}-deficient [p15(-/-)] MEFs treated with PD98059. The p15(-/-) MEFs exhibited decreased PD98059 sensitivity relative to wild-type MEFs (Fig. 5A). To analyze the physiologic relevance of the induction of p15^{INK4b} in ZD1839-induced growth inhibition, we next examined the effects of ZD1839 on the cell growth of wild-type and p15(-/-) MEFs. As expected, the p15(-/-) MEFs grew more rapidly than wild-type MEFs in the absence of ZD1839. The p15(-/-) MEFs were also more resistant to the growth inhibitory effects of ZD1839 than were wild-type MEFs, and 2 $\mu\text{mol/L}$ ZD1839 had a cytostatic effect in wild-type MEFs (Fig. 5B and C).

Furthermore, we found that ERK phosphorylation was inhibited in both types of MEFs; however, p15^{INK4b} protein induction by treatment with ZD1839 was detected only in wild-type MEFs (Fig. 5D).

To assess the influence of the activation status of ERK on ZD1839-mediated cell growth inhibition, we evaluated the antiproliferative effects of ZD1839 in two human colon cancer cell lines, HT-29 and Colo320DM (Fig. 6A). The graph shows that the growth of HT-29 cells was inhibited in a dose-dependent manner; however, that of Colo320DM cells was not inhibited by ZD1839. To investigate whether the difference in growth inhibition by ZD1839 between the two cell lines depends on ERK phosphorylation and p15^{INK4b} induction, we did Western

blot analysis. The level of ERK in Colo320DM cells was higher than that in HT-29 cells; however, constitutive phosphorylation of ERK was not observed in Colo320DM cells (Fig. 6B). Moreover, p15^{INK4b} induction and the inhibition of ERK phosphorylation by ZD1839 were detected only in HT-29 cells. Taken together, these results suggest that loss of p15^{INK4b} influences the cellular response to the antiproliferative effects of ZD1839 and that, in addition to induction of p15^{INK4b}, status of ERK phosphorylation and inactivation of the MAPK/ERK pathway play important roles in the cell growth inhibition induced by ZD1839.

Discussion

A great number of cancer studies have shown that the RB pathway is the most frequently inactivated in human malignant tumors (6, 7). If the RB pathway is inactivated, activation of the INK4 family leads to functional restoration of this pathway. Interestingly, it has been reported that ZD1839 induces p21^{WAF1} and p27^{KIP1} (32, 33) and imatinib mesylate (STI571, Gleevec) up-regulates p18^{INK4c} (34), resulting in hypophosphorylation of the RB protein.

In the present study, we disclosed that ZD1839 up-regulates p15^{INK4b} protein and subsequently converts a

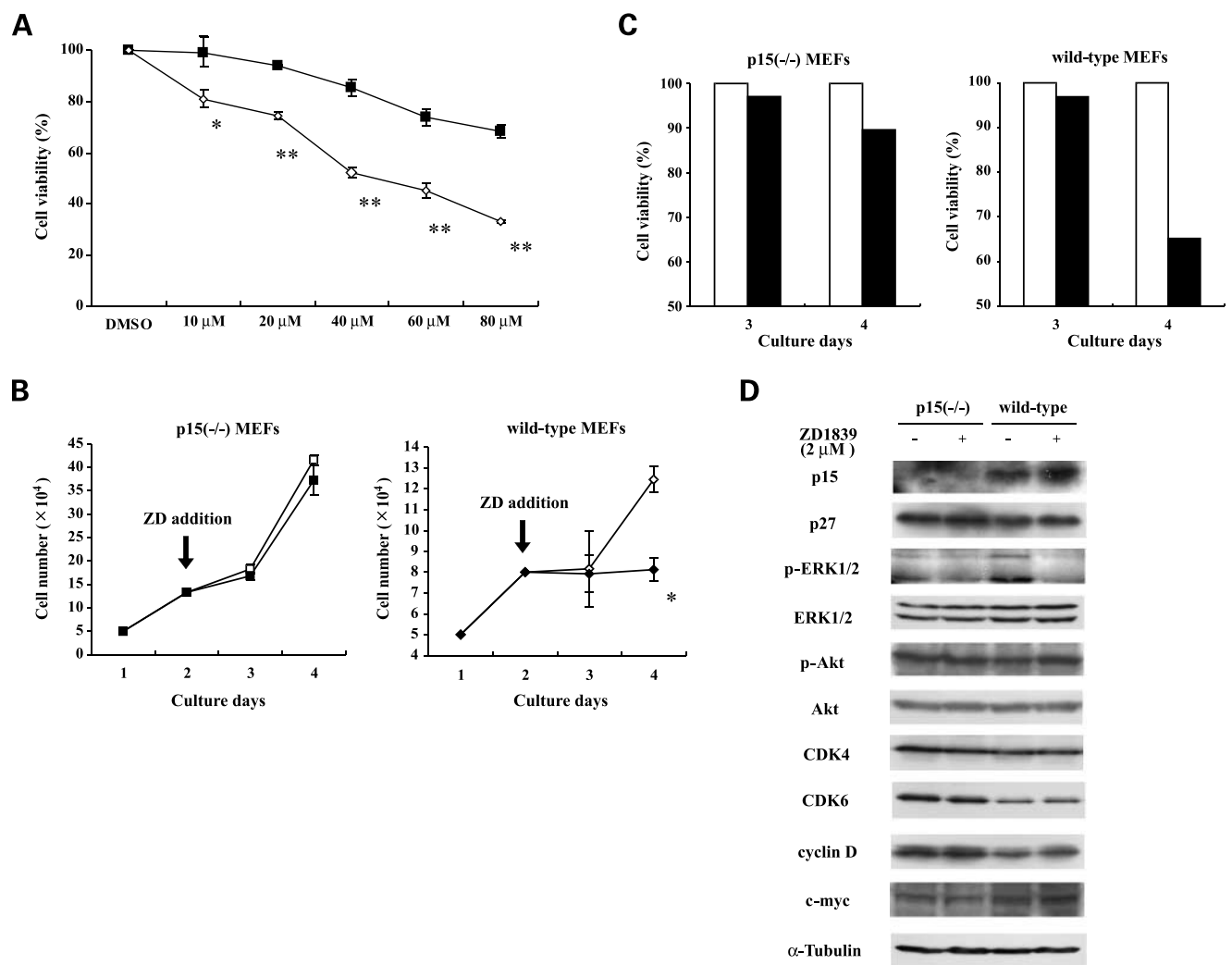


Figure 5. Effects of PD98059 and ZD1839 on the cell growth of wild-type and p15(-/-) MEFs. **A**, wild-type and p15(-/-) MEFs were treated with medium containing various concentrations of PD98059 for 4 d. Relative cell viabilities of wild-type (◇) or p15(-/-) (■) MEFs were counted by Cell Counting Kit-8 assay. Points, mean of triplicate experiments; bars, SD. *, $P < 0.05$ **, $P < 0.01$, significantly different between both MEF cell types. **B**, at 1 d after inoculation of p15(-/-) (left) and wild-type (right) MEFs, ZD1839 at 2 μmol/L (black column) was added, and cell growth was compared with control culture (white column). Points, mean of triplicate experiments; bars, SD. *, $P < 0.01$, significantly different compared with DMSO-treated control. **C**, relative cell viabilities of p15(-/-) (left) or wild-type (right) MEFs treated with 2 μmol/L ZD1839 (black columns) versus those that were untreated (white columns). **D**, both MEF cell types were exposed to DMSO (-) or 2 μmol/L ZD1839 (+) for 48 h. The expressions of p15^{INK4b}, p27^{KIP1}, p-ERK1/2, ERK1/2, p-Akt, Akt, CDK4/6, cyclin D1, and c-myc proteins were examined by Western blotting. α-Tubulin was chosen as the loading control in all blots.

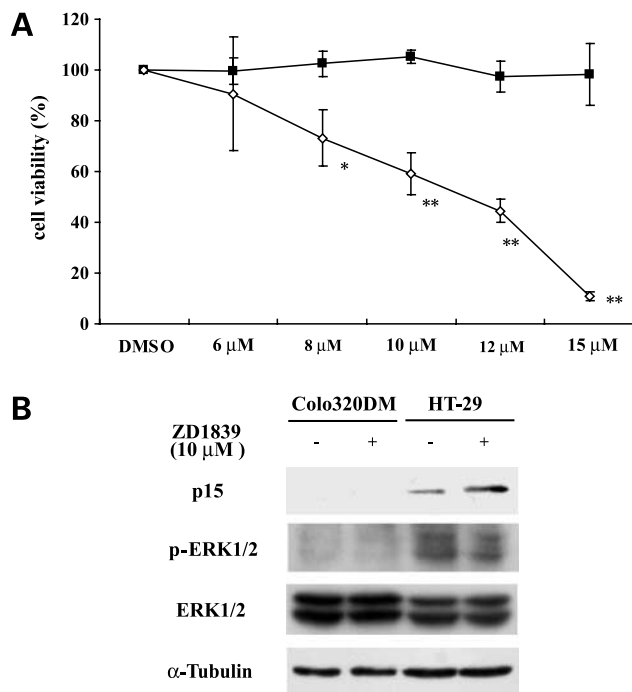


Figure 6. Effects of ZD1839 on the cell growth of human colon cancer Colo320DM and HT-29 cells. **A**, HT-29 and Colo320DM cells were treated with medium containing various concentrations of ZD1839 for 4 d. Relative cell viabilities of HT-29 (white column) or Colo320DM (black column) were counted by Cell Counting Kit-8 assay. Columns, mean of triplicate experiments; bars, SD. *, $P < 0.05$, **, $P < 0.01$, significantly different between both cells. **B**, HT-29 and Colo320DM cells were exposed to DMSO (-) or 10 μmol/L ZD1839 (+) for 48 h. The expressions of the p15^{INK4b}, p-ERK1/2, and ERK1/2 proteins were examined by Western blotting. α-Tubulin was chosen as the loading control in all blots.

hyperphosphorylated form of the RB protein into a hypophosphorylated form (Fig. 1C). Kiyota et al. (35) suggested that anti-EGFR mAb up-regulates p27^{KIP1} and p15^{INK4b} proteins and induces G₁ arrest in oral squamous carcinoma cell lines. Their report correlates with our result that the EGFR inhibitor ZD1839 increases p15^{INK4b} expression, arrests the cell cycle at the G₁ phase, and inhibits cell growth (Fig. 1). To further show that p15^{INK4b} induction through inhibition of ERK phosphorylation contributes to the antiproliferative activity of ZD1839, we did cell viability assays to assess the viability of wild-type and p15(-/-) MEFs treated with MEK inhibitor PD98059. We revealed that the p15(-/-) MEFs exhibited decreased PD98059 sensitivity relative to wild-type MEFs (Fig. 5A). Moreover, to emphasize the physiologic relevance of the induction of p15^{INK4b} in ZD1839-induced growth inhibition, we showed that loss of p15^{INK4b} was associated with resistance to ZD1839 (Fig. 5B and C). In addition, we showed that inhibition of ERK phosphorylation causes p15^{INK4b} induction (Fig. 4C). These results suggest that p15^{INK4b} induction through inhibition of the MAPK/ERK pathway is related to the antiproliferative effects of ZD1839. In contrast to our results, however, it was reported that activation of the Raf-MEK-ERK pathway involves p15^{INK4b} induction in some cell types (36, 37). This

difference may depend on particular properties of different cell lines.

Because we found that p15^{INK4b} mRNA is induced by ZD1839, we next investigated the molecular mechanism of p15^{INK4b} activation by ZD1839. To clarify whether the activation of the p15^{INK4b} promoter was responsible for the up-regulation of its mRNA, we examined the effects of ZD1839 on the promoter activity in a p15^{INK4b} promoter-luciferase fusion plasmid by transient assay. It was previously reported that transforming growth factor-β signaling induces p15^{INK4b} promoter activation by a combination of two coupled events: transactivation and relief of repression by c-myc (38). As a positive control, we showed that the p15^{INK4b} promoter was activated ~7.5-fold with 5.0 ng/μL transforming growth factor-β; however, we did not detect significant activation of the p15^{INK4b} promoter by ZD1839 (data not shown). Therefore, post-transcriptional mechanisms may be responsible for the induction of p15^{INK4b} by ZD1839.

We next revealed that stabilization of p15^{INK4b} mRNA could be associated with the up-regulation of p15^{INK4b} by ZD1839 (Fig. 2B). The regulation of mRNA stability is a central mechanism in the control of gene expression. It has been shown that adenylate/uridylate (AU)-rich elements (ARE), often containing one to several copies of the consensus sequence AUUUA, are critical *cis*-acting regulatory motifs located in the 3'-untranslated region of many mRNAs of cellular growth regulators, and that AREs are targets for *trans*-acting proteins to modulate mRNA stability (39). We found that the human p15 mRNA contains six separate AUUUA repeats in the 3'-untranslated region (Table 1). It has been shown that MAPK pathways, such as the c-jun NH₂-terminal kinase, p38, and ERK cascade, contribute to the stabilizing and destabilizing activities of ARE-binding factors in the regulation of half-lives of ARE-containing mRNAs (40, 41). Taken together, it could suggest that ZD1839 inhibition of the MAPK/ERK pathway may affect p15^{INK4b} mRNA stability through ARE-like sequences in the 3'-untranslated region.

Akt and ERK are important molecules of EGFR downstream signals because activation of the PI3K-Akt and MAPK/ERK pathways depends on the phosphorylation status of such signaling components in response to EGFR activation. Cappuzzo et al. (42) suggested that ZD1839 may

Table 1. RNA sequence of the human p15 mRNA 3'-untranslated region position sequence

Position	Sequence
-221-225, -228-232	... <u>UAAUUUAAU</u> UUUU
-1,053-1,057	...UU <u>UUUUAA</u> ...
-1,376-1,380	... <u>ACAUUUU</u> AU...
-1,409 to -1,413, -1,417 to -1,421	... <u>AAAUUUU</u> UAAA <u>UUUU</u>

NOTE: The ARE sequences are shown with AUUUA motifs underlined. The position numbers are derived from the human p15^{INK4b} cDNA sequence (GenBank).

be most effective against tumors with activated Akt; however, they found no correlation between activated ERK status and effectiveness of ZD1839. On the other hand, Ono et al. (43) indicated that high sensitivity to ZD1839 in cancer cell lines is closely correlated with dependence not only on Akt but also on ERK activation for cellular survival and proliferation. In our study, we showed that ZD1839 inhibited ERK phosphorylation but did not block Akt phosphorylation in HaCaT cells (Fig. 3). These results suggest that inhibition of ERK phosphorylation plays an important role in ZD1839-mediated cell cycle arrest. Furthermore, we found that the status of ERK phosphorylation and p15^{INK4b} induction through inhibition of ERK phosphorylation are involved in the antiproliferative activity of ZD1839 (Fig. 6A and B). Ogino et al. (30) reported that EGFR mutations are uncommon in colorectal cancer, and therefore other downstream molecules may influence responsiveness to EGFR inhibition. Taken together, our results may suggest that p15^{INK4b} induction through inhibition of ERK phosphorylation is associated with the antiproliferative effects of ZD1839.

Our results have suggested that ZD1839 induces p15^{INK4b} through inhibition of ERK phosphorylation, resulting in hypophosphorylation of the RB protein. Therefore, anticancer agents activating RB function, such as ZD1839, may contribute to new strategies for the therapy of malignancies, which we have termed "gene-regulating chemotherapy" (44, 45). A common strategy to detect a novel molecular-targeting anticancer agent has been based on finding direct inhibitors of various malignancy-related molecules in *in vitro* conditions. On the other hand, using the screening system we established, we were able to identify several p15^{INK4b}-inducing agents containing ZD1839. This suggests that INK4 family-inducing agents, toward activation of RB function, will be useful as new molecular-targeting anticancer drugs against malignant tumors.

Acknowledgments

We thank Dr. P. Krimpenfort for wild-type and p15^{INK4b}-deficient MEFs, and Dr. Y. Sowa for his helpful discussion and useful advice.

References

1. Massague J. G₁ cell-cycle control and cancer. *Nature* 2004;432:298–306.
2. Sherr CJ. Mammalian G₁ cyclins. *Cell* 1993;73:1059–65.
3. Dowdy SF, Hinds PW, Louie K, Reed SI, Arnold A, Weinberg RA. Physical interaction of the retinoblastoma protein with human D cyclins. *Cell* 1993;73:499–511.
4. Serrano M, Hannon GJ, Beach D. A new regulatory motif in cell-cycle control causing specific inhibition of cyclin D/CDK4. *Nature* 1993;366:704–7.
5. Hirai H, Roussel MF, Kato J, Ashmun RA, Sherr CJ. Novel INK4 proteins, p19 and p18, are specific inhibitors of the cyclin D-dependent kinases CDK4 and CDK6. *Mol Cell Biol* 1995;15:2672–81.
6. Roussel MF. The INK4 family of cell cycle inhibitors in cancer. *Oncogene* 1999;18:5311–7.
7. Irwin MS, Kaelin WG. p53 family update: p73 and p63 develop their own identities. *Cell Growth Differ* 2001;12:337–49.
8. Franklin DS, Godfrey VL, Lee H, et al. CDK inhibitors p18(INK4c) and p27(Kip1) mediate two separate pathways to collaboratively suppress pituitary tumorigenesis. *Genes Dev* 1998;12:2899–911.
9. Latres E, Malumbres M, Sotillo R, et al. Limited overlapping roles of P15^{INK4b} and P18^{INK4c} cell cycle inhibitors in proliferation and tumorigenesis. *EMBO J* 2000;19:3496–506.
10. Krimpenfort P, Quon KC, Mooi WJ, Loonstra A, Berns A. Loss of p16^{INK4a} confers susceptibility to metastatic melanoma in mice. *Nature* 2001;413:83–6.
11. Merlo A, Herman JG, Mao L, et al. 5' CpG island methylation is associated with transcriptional silencing of the tumour suppressor p16/CDKN2/MTS1 in human cancers. *Nat Med* 1995;1:686–92.
12. Esteller M, Corn PG, Baylin SB, Herman JG. A gene hypermethylation profile of human cancer. *Cancer Res* 2001;61:3225–9.
13. Hannon GJ, Beach D. p15^{INK4b} is a potential effector of TGF- β -induced cell cycle arrest. *Nature* 1994;371:257–61.
14. Tanaka T, Iwasa Y, Kondo S, Hiai H, Toyokuni S. High incidence of allelic loss on chromosome 5 and inactivation of p15^{INK4b} and p16^{INK4a} tumor suppressor genes in oxystress-induced renal cell carcinoma of rats. *Oncogene* 1999;18:3793–7.
15. Kurakawa E, Shimamoto T, Utsumi K, Hirano T, Kato H, Ohyashiki K. Hypermethylation of p16(INK4a) and p15(INK4b) genes in non-small cell lung cancer. *Int J Oncol* 2001;19:277–81.
16. Yokota T, Matsuzaki Y, Miyazawa K, Zindy F, Roussel MF, Sakai T. Histone deacetylase inhibitors activate INK4d gene through Sp1 site in its promoter. *Oncogene* 2004;23:5340–9.
17. Yokota T, Matsuzaki Y, Sakai T. Trichostatin A activates p18^{INK4c} gene: differential activation and cooperation with p19^{INK4d} gene. *FEBS Lett* 2004;574:171–5.
18. Hitomi T, Matsuzaki Y, Yokota T, Takaoka Y, Sakai T. p15^{INK4b} in HDAC inhibitor-induced growth arrest. *FEBS Lett* 2003;554:347–50.
19. Matsuzaki Y, Koyama M, Hitomi T, Kawanaka M, Sakai T. Indole-3-carbinol activates the cyclin-dependent kinase inhibitor p15^{INK4b} gene. *FEBS Lett* 2004;576:137–40.
20. Albanell J, Codony-Servat J, Rojo F, et al. Activated extracellular signal-regulated kinases: association with epidermal growth factor receptor/transforming growth factor α expression in head and neck squamous carcinoma and inhibition by anti-epidermal growth factor receptor treatments. *Cancer Res* 2001;61:6500–10.
21. Janmaat ML, Kruyt FA, Rodriguez JA, Giaccone G. Response to epidermal growth factor receptor inhibitors in non-small cell lung cancer cells: limited antiproliferative effects and absence of apoptosis associated with persistent activity of extracellular signal-regulated kinase or Akt kinase pathways. *Clin Cancer Res* 2003;9:2316–26.
22. Barnes CJ, Bagheri-Yarmand R, Mandal M, et al. Suppression of epidermal growth factor receptor, mitogen-activated protein kinase, and Pak1 pathways and invasiveness of human cutaneous squamous cancer cells by the tyrosine kinase inhibitor ZD1839 (Iressa). *Mol Cancer Ther* 2003;2:345–51.
23. Rusch V, Klimstra D, Venkatraman E, Pisters PW, Langenfeld J, Dmitrovsky E. Overexpression of the epidermal growth factor receptor and its ligand transforming growth factor α is frequent in resectable non-small cell lung cancer but does not predict tumor progression. *Clin Cancer Res* 1997;3:515–22.
24. Kersemaekers AM, Fleuren GJ, Kenter GG, et al. Oncogene alterations in carcinomas of the uterine cervix: overexpression of the epidermal growth factor receptor is associated with poor prognosis. *Clin Cancer Res* 1999;5:577–86.
25. Anderson NG, Ahmad T, Chan K, Dobson R, Bundred NJ. ZD1839 (Iressa), a novel epidermal growth factor receptor (EGFR) tyrosine kinase inhibitor, potentially inhibits the growth of EGFR-positive cancer cell lines with or without erbB2 overexpression. *Int J Cancer* 2001;94:774–82.
26. Arteaga CL. Epidermal growth factor receptor dependence in human tumors: more than just expression? *Oncologist* 2002;7:31–9.
27. Lynch TJ, Bell DW, Sordella R, et al. Activating mutations in the epidermal growth factor receptor underlying responsiveness of non-small-cell lung cancer to ZD1839. *N Engl J Med* 2004;350:2129–39.
28. Paez JG, Janne PA, Lee JC, et al. EGFR mutations in lung cancer: correlation with clinical response to ZD1839 therapy. *Science* 2004;304:1497–500.
29. Pao W, Miller V, Zakowski M, et al. EGF receptor gene mutations are common in lung cancers from "never smokers" and are associated with

- sensitivity of tumors to ZD1839 and erlotinib. *Proc Natl Acad Sci U S A* 2004;101:13306–11.
30. Ogino S, Meyerhardt JA, Cantor M, et al. Molecular alterations in tumors and response to combination chemotherapy with gefitinib for advanced colorectal cancer. *Clin Cancer Res* 2005;11:6650–6.
31. Sambrook J, Russell DW, editors. *Molecular cloning: a laboratory manual*. 1st ed. Cold Spring Harbor (NY): Cold Spring Harbor Laboratory Press; 2001. p. 7.42–4.
32. Janne PA, Taffaro ML, Salgia R, Johnson BE. Inhibition of epidermal growth factor receptor signaling in malignant pleural mesothelioma. *Cancer Res* 2002;62:5242–7.
33. Di Gennaro E, Barbarino M, Bruzzese F, et al. Critical role of both p27^{KIP1} and p21^{CIP1/WAF1} in the antiproliferative effect of ZD1839 (“Iressa”), an epidermal growth factor receptor tyrosine kinase inhibitor, in head and neck squamous carcinoma cells. *J Cell Physiol* 2003;195:139–50.
34. Nishimura N, Furukawa Y, Sutheesophon K, et al. Suppression of ARG kinase activity by STI571 induces cell cycle arrest through up-regulation of CDK inhibitor p18/INK4c. *Oncogene* 2003;22:4074–82.
35. Kiyota A, Shintani S, Mihara M, et al. Anti-epidermal growth factor receptor monoclonal antibody 225 up-regulates p27^{KIP1} and p15^{INK4B} and induces G₁ arrest in oral squamous carcinoma cell lines. *Oncology* 2002;63:92–8.
36. Malumbres M, Perez De Castro I, Hernandez MI, Jimenez M, Corral T, Pellicer A. Cellular response to oncogenic ras involves induction of the Cdk4 and Cdk6 inhibitor p15^{INK4b}. *Mol Cell Biol* 2000;20:2915–25.
37. Wen-Sheng W. ERK signaling pathway is involved in p15INK4b/p16INK4a expression and HepG2 growth inhibition triggered by TPA and Saikosaponin a. *Oncogene* 2003;22:955–63.
38. Seoane J, Poupnot C, Staller P, Schader M, Eilers M, Massagué J. TGF β influences Myc, Miz-1 and Smad to control the CDK inhibitor p15^{INK4b}. *Nat Cell Biol* 2001;3:400–9.
39. Shaw G, Kamen R. A conserved AU sequence from the 3' untranslated region of GM-CSF mRNA mediates selective mRNA degradation. *Cell* 1986;46:659–67.
40. Sirenko OI, Lofquist AK, DeMaria CT, Morris JS, Brewer G, Haskill JS. Adhesion-dependent regulation of an AU-rich element-binding activity associated with AUF1. *Mol Cell Biol* 1997;17:3898–906.
41. Sheng H, Shao J, DuBois RN. K-Ras-mediated increase in cyclooxygenase 2 mRNA stability involves activation of the protein kinase B. *Cancer Res* 2001;61:2670–5.
42. Cappuzzo F, Magrini E, Ceresoli GL, et al. Akt phosphorylation and gefitinib efficacy in patients with advanced non-small-cell lung cancer. *J Natl Cancer Inst* 2004;96:1133–41.
43. Ono M, Hirata A, Kometani T, et al. Sensitivity to gefitinib (Iressa, ZD1839) in non-small cell lung cancer cell lines correlates with dependence on the epidermal growth factor (EGF) receptor/extracellular signal-regulated kinase 1/2 and EGF receptor/Akt pathway for proliferation. *Mol Cancer Ther* 2004;3:465–72.
44. Sakai T. Molecular cancer epidemiology—the present status and future possibilities. *Jpn J Hygiene* 1996;50:1036–46.
45. Sowa Y, Sakai T. Butyrate as a model for “Gene-regulating chemoprevention and chemotherapy”. *Biofactors* 2000;2:283–7.